

Intra-arterial CECT of the Distal Forelimb in Jeju horses: Evaluating CE Factors

Seyoung Lee¹, Kwang-Yun Shin², Kija Lee³, and Jong-pil Seo¹

¹Jeju National University

²Jeju Provincial Government

³Kyungpook National University College of Veterinary Medicine

March 17, 2024

Abstract

Background: Few studies have investigated the adequate contrast enhancement (CE) evaluation depending on concentration, volume, and rate of contrast media (CM) and the scan parameters in equine contrast enhanced computed tomography (CECT). **Objectives:** We investigated CE of the deep digital flexor tendon (DDFT) and arteries depending on voltage, concentration, volume, and rate of CM during intra-arterial CECT of equine distal forelimbs. **Study design:** This is a prospective study. **Methods:** Six horses underwent fifty-four CT scans. First, the CE of DDFT and arteries was evaluated depending on the voltage (80 or 120 kV) and CM concentration (150, 120, or 90 mg I/mL in 50 mL of CM). Second, CE of DDFT and vessels was evaluated depending on the CM volume (50, 100, or 150 mL) and administration rate (2, 4, or 6 mL/s) with a fixed iodine delivery rate (IDR) (300 or 180 mg I/s). **Results:** CE of DDFT significantly increased at 80 kV of voltage and 150 mg I/mL of CM concentration (Median: 29.65; IQR: 1.74; $P < 0.05$). CE of the DDFT positively correlated with CM concentration ($P = 0.0004$; $r = 0.75$). At 180 mg I/s of IDR, an increase in rate and volume (6 mL/s and 150 mL) led to low contrast attenuation in the medial and lateral palmar arteries (median and IQR: 985.93 and 71.8 Hounsfield units [HU] and 988.73 and 41.16 HU, respectively); the CE was sufficient to distinguish the artery from the adjacent structures. **Main limitations:** The number of animals was small for parametric statistical analysis. **Conclusions:** Our results suggest that a low CM concentration could yield sufficient CE of the DDFT and arteries with adjusted CT scanning parameters or volume and injection rate of CM.

Introduction

Computed tomography (CT) is a valuable diagnostic modality for images of the musculoskeletal system, particularly for osseous changes. Recently, with technological developments, CT has been used to generate images of adequate quality to evaluate soft tissues, especially with contrast enhancement (CE) (Jones *et al.* , 2019, Pauwels *et al.* , 2021, Puchalski *et al.* , 2009, van Hamel *et al.* , 2014). Sunagawa *et al.* reported that three-dimensional CT images identified ruptures of the flexor tendon in the hand and wrist in human adults (Sunagawa *et al.* , 2003). Likewise, equine CT and contrast-enhanced CT (CECT) reportedly generate adequate images to reveal lesions in the deep digital flexor tendon (DDFT) (Jones *et al.* , 2019, van Hamel *et al.* , 2014, Vallance *et al.* , 2012), indicating that CT is an excellent modality to evaluate bone and soft-tissue lesions.

Jeju horse is a native breed of Jeju island in Korea, with a mean height and body weight are 123.72 cm and 267.00 kg, respectively (Oh *et al.* , 2014, Kong *et al.* , 2011). Since being used for racing, the number and value of Jeju horses have increased, resulting in an increase in admissions to equine hospitals. However, research on diseases or diagnostic modalities in these horses remains limited.

MRI is still considered a golden standard for evaluating the musculoskeletal system. However, considering the prolonged anaesthesia duration (Jone *et al.* , 2019) and facility limitation, CECT can be an alternative

diagnostic modality to MRI for assessing the equine distal limbs (Jones *et al.* , 2019, Puchalski *et al.* , 2007, Puchalski *et al.* , 2009, Puchalski 2012, van Hamel *et al.*,2014). To the best of our knowledge, no research has reported on the evaluation of CE in horses with different scanning parameters, concentrations, rates, and volumes of CM. In humans, low voltage and CM concentration can generate adequate CE to evaluate images in previous reports (Van Cauteren *et al.* , 2018). Several reports on CECT in horses used different CM concentrations (Puchalski *et al.* , 2007, Puchalski *et al.* , 2009, Puchalski *et al.* , 2017, Pauwels *et al.* , 2021, Vallance *et al.*, 2012 ^a and ^b, van Hamel *et al.*, 2014). In those reports, CM concentration, rate, and scanning parameters were 150-185 mg I/mL, 2-3 mL/s, and 120-140 kV, respectively. This report evaluated the CE of the DDFT and arteries using different CM concentrations, rates, volumes, and scanning parameters, providing practical information and the potential to use different scanning parameters and CM concentrations.

Material and methods

Animals

We scanned six healthy male Jeju horses without lameness (mean age: 3.83 ± 0.75 years; mean bodyweight: 281.17 ± 25.33 kg). Radiography of the bilateral forelimbs (from the carpal joint to the second pharynx) excluded horses with distal forelimbs abnormalities. We obtained two views of radiographs (lateral-medial view and dorso-palmar view). We only included horses without radiographic osseous changes. Complete blood counts were performed as pre-anesthetic evaluation. This study was approved by the Institutional Animal Care and Use Committee of OO University (2022-0046).

Design

This research was a prospective study. Each horse underwent nine CT scannings (Aquilion, Canon, Osaka, Japan) at >72 h intervals to avoid the effect of CM that had been previously injected. The experiments were conducted in two phases. First, we measured contrast attenuation of the DDFT and arteries depending on the scanning parameters (120 kV and 150 mA; 80 kV and 250 mA) and concentration of CM (150, 120, or 90 mg I/mL; Table 1). The injection rate of CM (Omnipaque 300; GE Healthcare, Chicago, IL) and the scan timing were 2 mL/s and 3 s, respectively. Two groups were selected for the second experiment, wherein, at a fixed IDR and total iodine dose (TID), contrast attenuation was measured depending on the volume and rate of CM (4 or 6 mL/s and 100 or 150 mL, respectively; Table 2). Scan parameters were set as 1 mm slice thickness and 0.75 sec rotation time, and the field of view was adjusted to include both limbs and from the carpal joint to the toe of limb of the interests in both phases.

Procedure

Each horse received detomidine hydrochloride (0.02 mg/kg, IV; Detomidin[®], Provet Veterinary Products Ltd., Istanbul, Turkiye), diazepam (0.03 mg/kg, IV; Diazepam inj., Samjin Pharm. Co. Ltd., Hwasung-si, Korea), and ketamine (2 mg/kg, IV; ketamin injection, Yuhan, Chungju-si, Korea) for sedation and anaesthesia induction. Anaesthesia was maintained with isoflurane (Ifran, Hana Pharm. Co. Ltd., Hwasung-si, Korea) and 100 % oxygen. The horses were placed in the left lateral recumbency position on the custom-made stationary table. An 18-gauge catheter was inserted aseptically into the medial palmar artery under the carpal joint under ultrasound guide. A pre-contrast CT was performed, followed by a CECT scan started 3 s after CM injection using a remote-control injector maximum pressure was set to 300 psi (Medrad[®] Slient S, Imaxeon Pty Lts. Rydalmere, Australia). Following CT scans, the intra-arterial catheter was removed, and a pressure bandage was applied. Horses received detomidine hydrochloride (0.1 mL, IV; Detomidin[®], Provet Veterinary Products Ltd., Istanbul, Turkiye) to prevent excitement and recovered from anaesthesia without assistance. The injector pressure (psi), volume of CT dose index ($CTDI_{vol}$), and anaesthesia time were recorded for each procedure.

Evaluation of CT images

The Hounsfield units (HU) were measured in the DDFT (Fig. 1) and medial and lateral palmar digital arteries (Fig. 2) at the following sites: the upper level of the proximal sesamoid bone (1); the lower level of the proximal

sesamoid bone (2); the middle level of the metacarpal bone (3); the level of the metacarpophalangeal joint (4). The region of interest (ROI) was manually drawn marginally for adjusting the size of the DDFT and arteries at the sites of interest. All the CT images were evaluated using a soft tissue algorithm (WW, 120 HU; WL, 400 HU), and reconstruction was performed with a 2 mm slice thickness and interval.

Statistical analysis

A Wilcoxon rank-sum test evaluated the difference between the HU of pre-contrast enhancement (HU_{pre}) and that of post-contrast enhancement (HU_{post}). We compared the mean HU in the DDFT and palmar arteries at each site, calculating the difference between HU_{pre} and HU_{post} ($HU_{post} - HU_{pre}$) of the DDFT. Statistical analyses were performed using the non-parametric Kruskal- wallis rank-sum test and Spearman's rank correlation analysis for assessing groups. A Wilcoxon rank-sum test was performed for the post-hoc test. The P value was adjusted using the Bonferroni method. Statistical significance was set at $P < 0.05$. All statistical analysis was processed using RStudio (RStudio, Boston, MA).

Results

The total duration of this study was 5 months. The second phase was conducted four weeks after the first phase. Tables 1 and 2 present the contrast attenuation of the DDFT and palmar arteries at each site. HU_{post} was significantly higher than HU_{pre} except for five measurements (site 3 in Group A, site 2 in Group B, site 3 in Group C, site 4 in Group F, and site 2 in Group G). Additionally, median HU_{post} was significantly higher than median HU_{pre} in all groups.

Contrast attenuation of the DDFT and arteries - First phase

The contrast attenuation values of the first phase are presented in Table 1. $HU_{post} - HU_{pre}$ of the DDFT was significantly different among groups ($P = 0.005$). Of the groups, group C (80 kV and 150 mg I/mL) showed significantly higher CE than other groups ($P < 0.05$). In 80 kV of voltage, $HU_{post} - HU_{pre}$ positively correlated with the concentration of CM ($P = 0.0004$, $r = 0.75$). A significant difference was observed only in the contrast enhancement of the medial palmar artery ($P = 0.008$). However, no specific groups showed a significant increase in contrast enhancement in the post-hoc analysis.

We then chose the concentration and scanning parameters of groups C and E, which showed significant CE of the DDFT and no differences among the other groups using low concentrations of CM. Accordingly, in the second study, CT was performed at 80 kV and 250 mA, while maintaining an iodine delivery rate (IDR) of 300 or 180 mg I/s. We scanned CT with different CM volumes and rates (4 or 6 mL/s and 100 or 150 mL).

Contrast attenuation of the DDFT and arteries – Second phase

Table 2 describes the attenuation values of the second phase. $HU_{post} - HU_{pre}$ of the DDFT showed significant differences among groups ($P = 0.0003$). Group C showed significantly higher CE ($P < 0.05$). With respect to palmar arteries, CE in medial and lateral palmar arteries showed significant differences among groups (medial: $P = 0.002$; lateral: $P = 0.001$). Group G showed a significantly lower in the CE than other groups, except for group F in the medial palmar artery and groups C and E in the lateral palmar artery ($P < 0.05$).

In 300 mg I/s of fixed IDR, volume and rate negatively correlated with $HU_{post} - HU_{pre}$ of the DDFT (volume: $P = 0.0002$, $r = -0.77$; rate: $P = 0.02$, $r = -0.54$). Conversely, a positive correlation was found between volume and CE of the medial and lateral palmar arteries (medial: $P = 0.02$, $r = 0.54$; lateral: $P = 0.03$, $r = 0.52$); the rate also showed a positive correlation with CE of the medial and lateral palmar arteries (medial: $P = 0.02$, $r = 0.54$; lateral: $P = 0.03$, $r = 0.52$). In 180 mg I/s of IDR, $HU_{post} - HU_{pre}$ of the DDFT showed a negative correlation with volume and rate (volume: $P = 0.003$, $r = -0.66$; rate: $P = 0.005$, $r = -0.63$). CE of the medial and lateral palmar arteries also showed negative correlation with volume and rate (volume: $P = 0.005$, $r = -0.63$ in the medial palmar artery and $P = 0.004$, $r = -0.64$ in the lateral palmar artery; rate: $P = 0.005$, $r = -0.63$ in the medial palmar artery and $P = 0.004$, $r = -0.64$ in the lateral palmar artery).

CTDI_{vol}, injector pressure, and anaesthesia time

Table 3 describes $CTDI_{vol}$, injector pressure, and anesthesia time for each group. The $CTDI_{vol}$ was 15.6 mGy and 8.5 or 9.4 mGy at high (120 kV and 150 mA) and low (80 kV and 250 mA) voltage, respectively. The remote-control injector measured the pressure injection from 45 to 118 psi. Correlation analysis revealed no significant differences between the concentration and pressure injections in the first phase. In the second phase, at 180 mg I/s of IDR, rate and volume positively correlated with pressure (rate: $r = 0.79$, $P = 0.0001$; volume: $r = 0.79$, $P = 0.0001$); CM concentration negatively correlated with pressure ($r = -0.79$, $P = 0.0001$). The mean anaesthesia time was 43.43+-10.02 min. All the horses recovered uneventfully after anaesthesia.

Intra-arterial catheterization

We mostly scanned the left forelimb; however, when catheterization in the left was unavailable, we scanned the right forelimb in left lateral recumbency due to facility limitations - five of fifty-four CT scans. In the first phase, after one CT scan, one horse experienced damage to the left artery; however, ultrasound during the second phase revealed recovery of the artery after three months. In the second phase, ultrasonography identified a damaged left medial palmar artery after a CT scan of 300 mg I/s of IDR at a rate of 6 mL/s, wherein the maximal pressure was 118 psi. The horse showed no soft-tissue edema or lameness following CT scans. The other horses did not show any complications associated with intra-arterial catheterization.

Discussion

In this study, we found a significant increase in the mean value of CE in HU of the DDFT in all scans. Specifically, 150 mg I/mL of CM concentration and 2 mL/s of rate in conjunction with 80 kV yielded significantly higher CE of the DDFT than other conditions, corresponding to the fact that iodine makes higher CE at low voltage by its nature (Bae, 2010). In horses, voltages and CM concentrations for intra-arterial CECT in distal limbs were reportedly 120 or 140 kV and over 150 mg I/mL, respectively (Puchalski *et al.*, 2009 van Hamel *et al.*, 2014, Puchalski *et al.*, 2007, Vallance *et al.*, 2012a and b, Pauwels *et al.*, 2021). We scanned intra-arterial CECT using the same or lower voltage and concentration of CM, resulting in the CE of the DDFT not being significantly different from each other except for the scans using 80 kV and 150 mg I/mL. Considering these results, we suggest that 120 mg I/mL of 90 mg I/mL of CM might be applied for intra-arterial CECT of the distal limbs to yield CE of the DDFT in horses.

In the first phase, CE of the DDFT was positively correlated with CM concentration. However, in fixed IDR and total iodine dose (TID), volume and rate of CM negatively correlated with CE of the DDFT, indicating high CM concentration and low volume and rate efficiently yield CE of the DDFT in fixed IDR. Previously, Benrendt *et al.* reported that the volume and rate of CM administered intravenously did not affect a significant change in CE in abdominal soft tissues in fixed IDR (Behrendt *et al.*, 2008). Additionally, in experimental models using a constant CM concentration with a fixed injection duration, hepatic enhancement proportionally increased with an elevation of rate [?] 2 mL/s (Bae *et al.*, 1998), demonstrating that an increase in the velocity of injection over 2 mL/s slightly increased the CE of the liver. Although we administered CM intra-arterially in this study, the CE of the DDFT revealed a negative correlation with the rate and volume of CM at a fixed IDR. We assumed that it could be caused by the administration route and CM concentration; or because CE of tendons mainly occur through extravasation or neo-vascularization. Therefore, in fixed IDR or TID, we suggest that CE of the DDFT could efficiently be achieved at a high CM concentration with a slow rate (< 4 mL/s).

CM volume reportedly influences the CE of vessels (Ahmed *et al.*, 2009, Van Cauteren *et al.*, 2018). Van Cauteren *et al.* reported that the combination of high volume and low CM concentration yielded significantly higher HU with constant IDR in intravenous CECT (Van Cauteren *et al.*, 2018). Additionally, in intra-arterial CECT of canine models, CM volume was the most influential scan parameter for contrast enhancement (Ahmed *et al.* 2009). In this study, with 180 mg I/mL of IDR, the combination of 30 mg I/mL of concentration and 150 mL of large volume resulted in a significant decrease in CE of the arteries. The mean HU of arteries showed no decline in the condition of 45 mg I/mL of CM concentration with 100 mL of volume. Considering these results, large volumes might not result in higher CE of the arteries when CM

concentration is < 45 mg I/mL in intra-arterial CECT of equine distal limbs.

Volume and rate positively correlated with the CE of arteries; conversely, CM concentration negatively correlated with the CE of arteries during maintaining 300 mg I/s of IDR, coordinating with a previous study (Van Cauteren *et al.*, 2018). However, with 180 mg I/s of IDR, all parameters showed negative correlations with the CE of arteries. We presumed that 30 mg I/mL of low CM concentration yielded significantly low CE, causing the negative correlations. Van Cauteren *et al.* reported that in 0.64 g/s of constant IDR, CM concentration negatively correlated with CE of the aorta, central vena cava, and hepatic parenchyma in intra-venous CECT (Van Cauteren *et al.*, 2018). Our results also suggested that low CM concentration in conjunction with volume or rate adjustment with a certain fixed IDR could generate adequate CE in the arteries in the equine distal limbs

Concerning CM administration, the max pressure is reportedly below 150 psi (Pollard and Puchalski, 2011, Indrajit *et al.*, 2015). Previously, under constant IDR and TID, the rate had a greater impact on maximal pressure than viscosity (Van Cauteren *et al.*, 2018), indicating that in 180 mg I/s of IDR, the pressure positively correlated with the rate in this report. Pollard and Puchalski reported that for intra-arterial CECT of the equine distal limbs, the rate of CM injection is usually set at 2 mL/s using an 18-gauge catheter to minimize hemodynamic changes (Pollard and Puchalski, 2011). In this study, CM was administered at 2, 4, and 6 mL/s of rate. In a horse during the scan with 6 mL/s of rate and 300 mg I/s of IDR, the maximal pressure was 118 psi, causing no failure of the CE of the scan. However, during the following scan, an ultrasound revealed the damaged arteries; the horse showed no lameness or swelling in the region. Although 118 psi of the maximal pressure contributed to outcome, we considered that repeated catheterization, the patient's physiologic status, the integrity of the vascular wall, or vascular spasm could also have been potential causes.

In neck CT using phantom models, 80 kV of CT resulted in a decrease in radiation dose while maintaining the subjective image quality (Hoang *et al.*, 2012). Additionally, Gnannt *et al.* reported that 70 kV of CT showed no significantly different image quality of soft tissue in a cervical scan compared to that of a 120 kV scan (Gnannt *et al.*, 2012). Despite not evaluating the image quality of 80 kV and 120 kV CT scans, CTDI_{vol} in 80 kV scans was lower than that of 120 kV scans. In equine imaging, standing head CT scans are widely used, and little research on standing distal limb CT has been reported (Brounts *et al.*, 2022, Mageed 2020, Mathee *et al.*, 2023). Considering the future of CT scans without general anesthesia, human intervention during CT scans is inevitable, raising concerns against radiation doses. Therefore, further research on radiation dose reduction is required while maintaining diagnostic image quality in horses.

This study had several limitations. First, the number of animals was small for parametric statistical analysis. Second, the animals had no lesions in the distal limbs; thus, further research on CECT in horses with lesions is required. Third, we only conducted a CT scan of Jeju horses, which may have influenced CE. However, considering that we injected CM via intra-arterial catheterization, body size hardly affected CE. Fourth, we scanned the right limb only five times instead of the left due to the stationary facility and compromised left medial palmar artery.

We demonstrated contrast attenuation of the DDFT and palmar digital artery in the equine forelimb, depending on the scanning parameters, concentration, rate, and volume of CM administration. We found that the contrast attenuation of DDFT was significantly higher at low voltage (80 kV) and high CM concentrations (150 mg I/s); > 900 HU contrast attenuation of the artery was statistically lower at a low IDR (180 mg I/s) with a high CM rate (6 mL/s). Most horses did not show complications associated with intra-arterial injection following CT scans with a [?] 4 mL/s rate. This study provides practical information on the scan parameters and CM injection in equine intra-arterial CECT, the evaluation of equine distal limbs, and the anatomical features of CECT in Jeju horses.

Reference

Ahmed AS, Deuerling-Zheng Y, Strother CM, Pulfer KA, Zellerhoff M, Redel T, Royalty K, Consigny D, Lindstrom MJ, Niemann DB Impact of intra-arterial injection parameters on arterial, capillary, and venous

time-concentration curves in a canine model. *AJNR Am J Neuroradiol.* 2009;30(7):1337-41. yangsigyi maen wi

Bae KT, Heiken JP, Brink JA Aortic and hepatic peak enhancement at CT: effect of contrast medium injection rate—pharmacokinetic analysis and experimental porcine model. *Radiology.* 1998; 206(2):455-464.

Bae KT Intravenous contrast medium administration and scan timing at CT: considerations and approaches. *Radiology.* 2010.;256(1):32-61.

Brounts SH, Lund JR, Whitton RC, Ergun DL, Muir P Use of a novel helical fan beam imaging system for computed tomography of the distal limb in sedated standing horses: 167 cases (2019-2020). *J Am Vet Med Assoc.* 2022; 260(11):1351-1360.

Gnannt R, Winklehner A, Goetti R, Schmidt B, Kollias S, Alkadhi H Low kilovoltage CT of the neck with 70 kVp: comparison with a standard protocol. *AJNR Am J Neuroradiol.* 2012; 33(6):1014-1019.

Hoang JK, Yoshizumi TT, Nguyen G, Toncheva G, Choudhury KR, Gafton AR, Eastwood JD, Lowry C, Hurwitz LM Variation in tube voltage for adult neck MDCT: effect on radiation dose and image quality. *AJR Am J Roentgenol.* 2012; 198(3):621-627.

Indrajit IK, Sivasankar R, D'Souza J, Pant O, Negi RS, Sahu S, PI H Pressure injectors for radiologists: A review and what is new. *Indian J Radiol Imaging.* 2015; 25(1):2-10.

Jones ARE., Ragle CA, Mattoon JS, Sanz MG Use of non-contrast-enhanced computed tomography to identify deep digital flexor tendinopathy in horses with lameness: 28 cases (2014-2016). *J Am Vet Med Assoc.* 2019; 254(7):852-858.

Kong HS, Lee HK, Park KD, Choi BW A breed comparison on the finishing times of racehorses. *J Anim Sci Technol.* 2011; 53(1): 23–27.

Mathee N, Robert M, Higgerty SM, Fosgate GT, Rogers AL, d'Ablon X, Carstens A Computed tomographic evaluation of the distal limb in the standing sedated horse: Technique, imaging diagnoses, feasibility, and artifacts. *Vet Radiol Ultrasound.* 2023; 64(2):243-252.

Mathee N, Robert M, Higgerty SM, Fosgate GT, Rogers AL, d'Ablon X, Carstens A Computed tomographic evaluation of the distal limb in the standing sedated horse: Technique, imaging diagnoses, feasibility, and artifacts. *Vet Radiol Ultrasound.* 2023; 64(2):243-252.

Oh WY, Kim BW, Cho HW, Shin TS, Cho SK, Cho BW Analysis of associated race performance and functional characterization of conformation in Jeju horse. *J Agric Life Sci.* 2014; 48(1):99–106.

Pauwels F, Hartmann A, Alawneh J, Wightman P, Saunders J Contrast Enhanced Computed Tomography Findings in 105 Horse Distal Extremities. *J Equine Vet Sci.* 2021; 104:103704.

Pollard R, Puchalski S CT contrast media and applications, in: Schwarz T., Saunders J. (the 1st Ed.), *Veterinary Computed tomography.* John Wiley & Sons. Ltd. New Jersey. 2011; pp. 57–65.

Puchalski SM Advances in equine computed tomography and use of contrast media. *Vet Clin North Am Equine Pract.* 2012; 28(3):563-81.

Puchalski SM, Galuppo LD, Hornof WJ, Wisner ER Intraarterial contrast-enhanced computed tomography of the equine distal extremity. *Vet Radiol Ultrasound.* 2007; 48(1):21-29.

Puchalski SM, Galuppo LD, Drew CP, Wisner ER Use of contrast-enhanced computed tomography to assess angiogenesis in deep digital flexor tendonopathy in a horse. *Vet Radiol Ultrasound.* 2009; 50(3):292-297.

Solbak MS, Henning MK, England A, Martinsen AC, Aalokken TM, Johansen S Impact of iodine concentration and scan parameters on image quality, contrast enhancement and radiation dose in thoracic CT. *Eur Radiol Exp.* 2020; 11;4(1):57.

Sunagawa T, Ochi M, Ishida O, Ono C, Ikuta Y Three-dimensional CT imaging of flexor tendon ruptures in the hand and wrist. *J Comput Assist Tomogr.* 2003; 27(2):169-74.

Vallance SA, Bell RJ, Spriet M, Kass PH, Puchalski SM Comparisons of computed tomography, contrast enhanced computed tomography and standing low-field magnetic resonance imaging in horses with lameness localised to the foot. Part 1: anatomic visualisation scores. *Equine Vet J.* 2012a; 44(1):51-56.

Vallance SA, Bell RJW, Spriet M, Kass PH, Puchalski SM Comparisons of computed tomography, contrast enhanced computed tomography and standing low-field magnetic resonance imaging in horses with lameness localized to the foot. Part 2: Lesion identification. *Equine Vet J.* 2012b; 44:144–156.

Van Cauteren T, Van Gompel G, Nieboer KH, Willekens I, Evans P, Macholl S, Droogmans S, de Mey J, Buls N Improved enhancement in CT angiography with reduced contrast media iodine concentrations at constant iodine dose. *Sci Rep.* 2018; 30;8(1):17493.

van Hamel SE, Bergman HJ, Puchalski SM, de Groot MW, van Weeren PR Contrast-enhanced computed tomographic evaluation of the deep digital flexor tendon in the equine foot compared to macroscopic and histological findings in 23 limbs. *Equine Vet J.* 2014; 46(3):300-5.

Acknowledgements

Authors would like to appreciate staffs of OO Equine Hospital for supporting the process of this study. Also, we would like to thank Editage (www.editage.co.kr) for English language editing.

Group	Group	A	B	C
Scanning parameters	Scanning parameters	120 kV and 150 mA	120 kV and 150 mA	80 kV and 250 mA
Iodine concentration	Iodine concentration	150 mg I/mL	120 mg I/mL	150 mg I/mL
	Site			
HU_{pre}	1	83.37±5.32	87.5±8.42	85.05±13.85
	2	82.82±10.81	87.96±4.8	84.1±10.26
	3	104.95±23.75	102.47±6	99.16±16.19
	4	109.51±15.57	108.92±7.59	110.66±18.2
HU_{post}	1	111.2±10.44**	107.01±6.8**	113.38±10.26**
	2	100.39±8.2**	98.12±15.07	116.63±11.59**
	3	119.26±20.4	122.56±6.9**	125.47±22.65*
	4	127±16.59*	120.54±9.77*	136.89±20.1*
HU_{med}	1	1284.16±175.18	1092.88±8.59	1151.64±113.7
	2	1200.25±61.89	1109.09±84.42	1163.52±42.43
	3	1269.14±148	1194.16±49.94	1321.52±154.49
	4	1260.4±156.01	1134.68±148.32	1177.59±26.63
HU_{lat}	1	1145.73±160.02	1126.2±92.64	1173.73±119.67
	2	1119.37±121.72	1123.04±104.98	1194.14±165.77
	3	1256.5±108.57	1256.9±134.87	1173.33±214.02
	4	1092.97±133.35	1164.62±142.19	1103.25±108.12
median HU_{pre}	median HU_{pre}	94.66±12.91	96.7±7.14	92.22±11.46
median HU_{post}	median HU_{post}	114.31±14.36**	114.79±11.54**	123.84±15.66**
median HU_{post}-HU_{pre}	median HU_{post}-HU_{pre}	20.21±3.81	16.1±7.68	29.65±1.74*
median HU_{med}	median HU_{med}	1282.07±99.8	1127.14±44.63	1210.22±43.84
median HU_{lat}	median HU_{lat}	1160.42±113.25	1170.57±53.73	1157.16±162.66

Table 1. Median ± IQR of Hounsfield unit (HU) measurements of the first study-Adjustment of scanning voltage and iodine concentration

In all groups, contrast medium (CM) volume, injection rate, and scanning timing were total 50 mL, 2 mL/s,

and 3 s after CM injection, respectively; HU_{pre} : pre-contrast attenuation of the deep digital flexor tendon (DDFT). HU_{post} : post-contrast attenuation of the DDFT. HU_{med} : post-contrast attenuation of the medial palmar artery (PA). HU_{lat} : post-contrast attenuation of the lateral PA. median HU_{pre} : Median of HU_{pre} ; median HU_{post} : median of HU_{post} ; median $HU_{post}-HU_{pre}$: median of the difference between HU_{pre} and HU_{post} ; median HU_{med} : Median of HU_{med} ; median of HU_{lat} : median of HU_{lat} . * $P < 0.05$; ** $P < 0.01$

Table 2. Median \pm IQR of HU measurements of the second study-Adjustment of volume, rate, and iodine delivery rate (IDR) of contrast medium (CM)

Group	Group	E	E	F	F
IDR	IDR	180 mg I/s	180 mg I/s	180 mg I/s	180 mg I/s
CM volume	CM volume	50 mL	50 mL	100 mL	100 mL
Injection rate	Injection rate	2 mL/s	2 mL/s	4 mL/s	4 mL/s
	Site				
HU_{pre}	1	86.4 \pm 4.07	86.4 \pm 4.07	92.05 \pm 4.77	92.05 \pm 4.77
	2	87.15 \pm 6.33	87.15 \pm 6.33	89.32 \pm 2.76	89.32 \pm 2.76
	3	106.04 \pm 9.28	106.04 \pm 9.28	100.18 \pm 4.27	100.18 \pm 4.27
	4	113.66 \pm 9.49	113.66 \pm 9.49	110.96 \pm 10.11	110.96 \pm 10.11
HU_{post}	1	110.47 \pm 13.97**	110.47 \pm 13.97**	102.64 \pm 3.97**	102.64 \pm 3.97**
	2	104.22 \pm 5.5**	104.22 \pm 5.5**	105.23 \pm 2.01**	105.23 \pm 2.01**
	3	124.91 \pm 9.76**	124.91 \pm 9.76**	116.29 \pm 6.44**	116.29 \pm 6.44**
	4	132.32 \pm 4.28**	132.32 \pm 4.28**	122.16 \pm 6.54	122.16 \pm 6.54
HU_{med}	1	1233.79 \pm 105.8	1233.79 \pm 105.8	1300.76 \pm 171.07	1300.76 \pm 171.07
	2	1196.8 \pm 123.62	1196.8 \pm 123.62	1271.11 \pm 95.21	1271.11 \pm 95.21
	3	1271.2 \pm 140.76	1271.2 \pm 140.76	1377.72 \pm 93.19	1377.72 \pm 93.19
	4	1282.25 \pm 117.83	1282.25 \pm 117.83	1309 \pm 112.86	1309 \pm 112.86
HU_{lat}	1	1154.41 \pm 59.87	1154.41 \pm 59.87	1084.04 \pm 188.53	1084.04 \pm 188.53
	2	1176.14 \pm 79.91	1176.14 \pm 79.91	1174.37 \pm 286.55	1174.37 \pm 286.55
	3	1184.11 \pm 110.88	1184.11 \pm 110.88	1219.16 \pm 225.21	1219.16 \pm 225.21
	4	1108.27 \pm 32.75	1108.27 \pm 32.75	1209.79 \pm 36.62	1209.79 \pm 36.62
median HU_{pre}	median HU_{pre}	97.28 \pm 4.97	98.21 \pm 4.23	98.21 \pm 4.23	95.65 \pm 6.21
median HU_{post}	median HU_{post}	117.62 \pm 7.12**	112.15 \pm 2.35**	112.15 \pm 2.35**	106.95 \pm 4.15**
median $HU_{post}-HU_{pre}$	median $HU_{post}-HU_{pre}$	18.42 \pm 6.58	12.56 \pm 3.88	12.56 \pm 3.88	12.61 \pm 2.32
median HU_{med}	median HU_{med}	1223.12 \pm 183.06	1333.51 \pm 109.76	1333.51 \pm 109.76	985.93 \pm 71.07
median HU_{lat}	median HU_{lat}	1135.04 \pm 87.86	1149.55 \pm 186.77	1149.55 \pm 186.77	972.89 \pm 41.10

In all groups, scanning parameters were 80 kV and 250 mA; HU_{pre} : pre-contrast attenuation of the deep digital flexor tendon (DDFT). HU_{post} : post-contrast attenuation of the DDFT. HU_{med} : post-contrast attenuation of the medial palmar artery (PA). HU_{lat} : post-contrast attenuation of the lateral PA. median HU_{pre} : Median of HU_{pre} ; median HU_{post} : median of HU_{post} ; median $HU_{post}-HU_{pre}$: median of the difference between HU_{pre} and HU_{post} ; median HU_{med} : Median of HU_{med} ; median of HU_{lat} : median of HU_{lat} . * $P < 0.05$; ** $P < 0.01$

Table 3. Visibility, the volume of CT dose index, injector pressure, and anesthesia time

Group	kV	Contrast medium	Contrast medium	Contrast medium	Contrast medium	Contrast medium	CTDI _{vol} (mGy)	Injector pressure (psi)	Anesthesia time (min)
		IDR (mg I/s)	Volume (mL)	Rate (mL/s)	Concentration (mg I/mL)	Total iodine dose (g)			

Group	kV	Contrast medium	CTDI _{vol} (mGy)	Injector pressure (psi)	An				
A	120	300	50	2	150	7.5	15.6	66.5±5.86	51.
B	120	240	50	2	120	6	15.6	67.3±11.02	46.
C	80	300	50	2	150	7.5	9.4	63.5±9.09	46.
D	80	240	50	2	120	6	9.4	58.67±13.75	40.
E	80	180	50	2	90	4.5	9.35	53.83±5.04	51.
F	80	180	100	4	45	4.5	9.4	59.83±6.59	37.
G	80	180	150	6	30	4.5	9.4	75.67±10.84	39.
H	80	300	100	4	75	7.5	9.25	61.5±9.78	40.
I	80	300	150	6	50	7.5	9.4	78.83±19.28	37.

IDR: Iodine delivery rate (mg I/s); CTDI_{vol} (mGy): the volume of CT dose index.

Figure legends

Figure 1. Measurements of Hounsfield unit (HU) of the deep digital flexor tendon (DDFT) at four sites: (1) the upper level of the proximal sesamoid bone; (2) the lower level of the proximal sesamoid bone; (3) the mid-level of the proximal phalangeal bone; and (4) the level of proximal phalangeal joint.

Figure 2. Measurements of Hounsfield unit (HU) of the artery. The HU of the medial and lateral palmar digital artery was measured at four sites: the upper level of the proximal sesamoid bone (1); the lower level of the proximal sesamoid bone (2); the mid-level of the proximal phalangeal bone (3); and the level of proximal phalangeal joint (4).

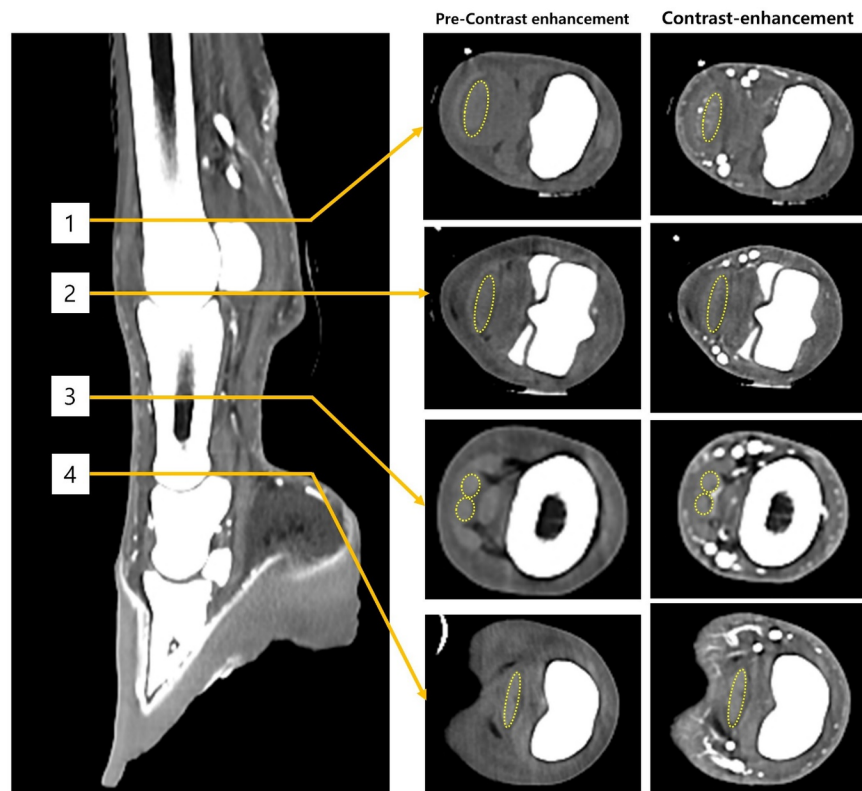


Figure 1.

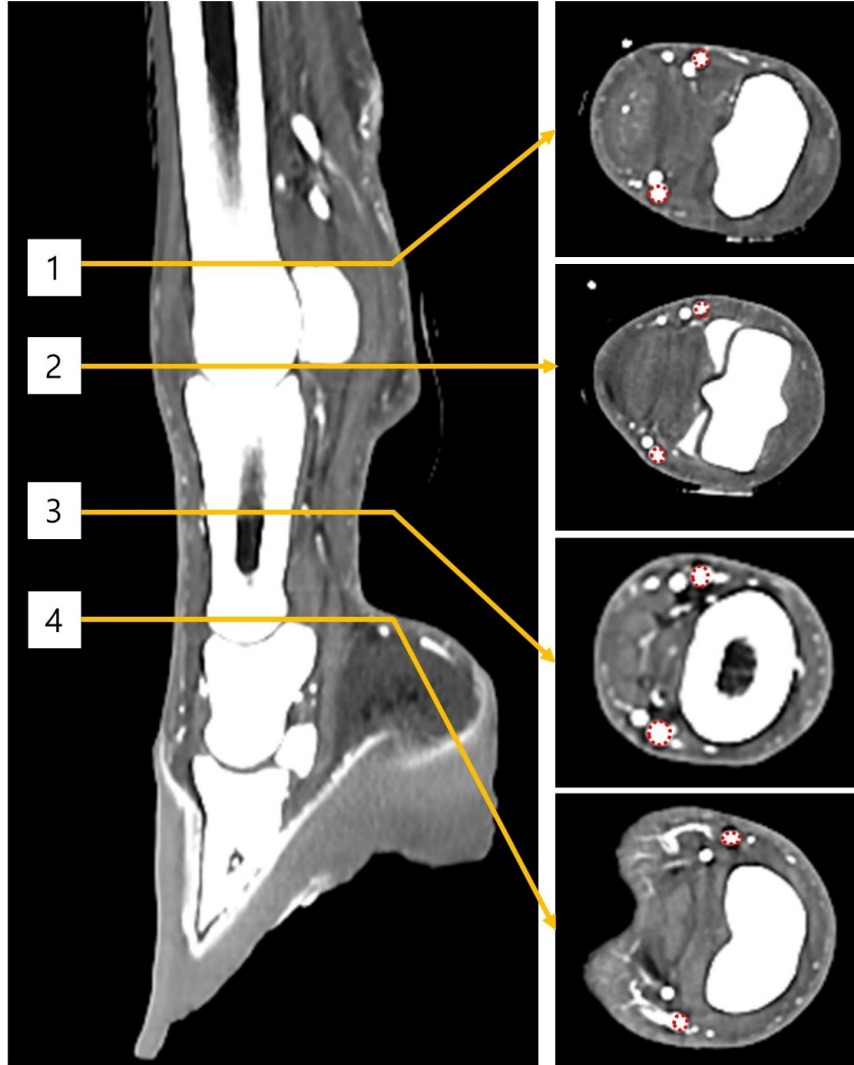


Figure 2.

